European Conference on Optical Communication © Optica Publishing Group 2022

Generalized Raman Scattering Model and Its Application to Closed-Form GN Model Expressions Beyond the C+L Band

C. Lasagni(1), P. Serena(2), A. Bononi(2), J-C. Antona(3)

(1)Università dell'Aquila, Dip. Scienze Fisiche e Chimiche, 67100 L'Aquila (Italy)
(2)Università di Parma, Dip. Ingegneria e Architettura, 43124 Parma (Italy) ✉ paolo.serena@unipr.it
(3)Alcatel Submarine Networks, 91620 Nozay (France)

Abstract *We derive a wide-band approximation of the stimulated Raman scattering formula and show its application to Gaussian noise (GN) model closed-form expressions for transmissions even beyond the C+L band.* © 2022 The Author(s)

Introduction

Optical systems exploiting multi-band transmissions represent an appealing technique in terms of potentially offered capacity[1]. For such systems, quick analytical tools to assess the system performance in the presence of wide-band effects such as stimulated Raman scattering (SRS)[2] are crucial to avoid extremely time-consuming numerical simulations[3], and for real-time management and optimization of an optical network[4],[5]. To this aim, the Gaussian noise (GN) model[6],[7] for the estimation of the fiber nonlinear interference (NLI) variance was extended to include SRS in[8],[9].

An SRS-aware closed-form GN model was derived in[10] by using the Christodoulides-Zirngibl SRS formula[11],[12] that postulates the Raman gain as linear in frequency with a frequency-independent loss. While a linear approximation is justified when the wavelength division multiplexing (WDM) bandwidth is below ≈15 THz, i.e., up to the C+L band, it over-estimates the Raman gain for larger bandwidths. To overcome this limitation, extended closed-form formulas based on fitting parameters have been proposed in[13],[14].

By leveraging a triangular approximation of the Raman gain, we propose a simple extension of the SRS model in[11],[12], which enables a generalization of the GN model formulas in[10] to multi-band transmissions even beyond C+L band.

Theory

The evolution along the fiber-optic distance z of the ith WDM channel power P_i is governed by the following ordinary differential equation (ODE)[2]

$$\frac{dP_i}{dz} = -P_i \sum_{j=1}^{i-1} \frac{\nu_j}{\nu_i} \tilde{g}_R(|f_i - f_j|) P_j \qquad (1)$$
$$+ P_i \sum_{j=i+1}^{N} \tilde{g}_R(|f_i - f_j|) P_j - \alpha(f_i) P_i$$

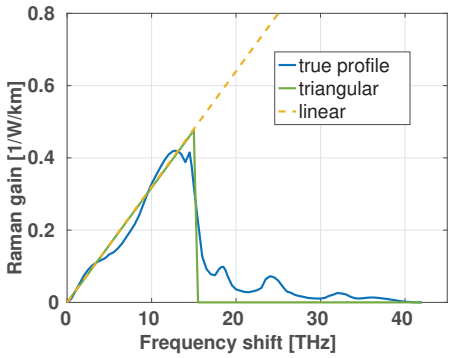

Fig. 1: Raman gain profile (interpolated from[2]) vs frequency shift with linear fitting[11],[12], and triangular approximation[15] imposing zero gain after a cut-off shift $\Delta f_{\rm co}$.

where ν_i is the carrier frequency of the ith channel, f_i is its low-pass frequency in a reference system centered at the WDM central frequency, N is the number of channels, α is the fiber loss coefficient, and $\tilde{g}_R$ is the Raman gain, as reported in Fig. 1.

An analytical solution for the ODE was proposed in[11],[12] by assuming $\nu_j/\nu_i \approx 1$, approximating the fiber loss with a constant value $\alpha(f) \equiv \overline{\alpha}$, and the Raman gain with a *linear* function of the frequency shift Δf, namely $\tilde{g}_R(\Delta f) \approx C_{\rm r} \Delta f$. Under these assumptions, Eq. (1) was solved in[11],[12] obtaining for P_i, $i = 1, \ldots, N$:

$$P_i(z) = P_i(0) \frac{e^{-C_{\rm r} L_{\rm eff}(z) r(f_i) - \overline{\alpha} z} P_{\rm t}}{\sum_{k=1}^{N} P_k(0) e^{-C_{\rm r} L_{\rm eff}(z) r(f_k)}} \qquad (2)$$

where: $P_{\rm t} = \sum_k P_k$ is the total power of the WDM signal, while $L_{\rm eff}(z) = (1 - e^{-\overline{\alpha} z})/\overline{\alpha}$ is the fiber effective length. The function $r(f)$ expresses the SRS shaping profile and, under the linear approximation of the Raman gain (see Fig. 1), is $r(f) = P_{\rm t} f$ at *any* frequency f.

Figure 1 suggests that such a linear approximation is justified when the maximum frequency shift between channels is less than ≈15 THz, as the Raman gain starts to vanish at wider spac-

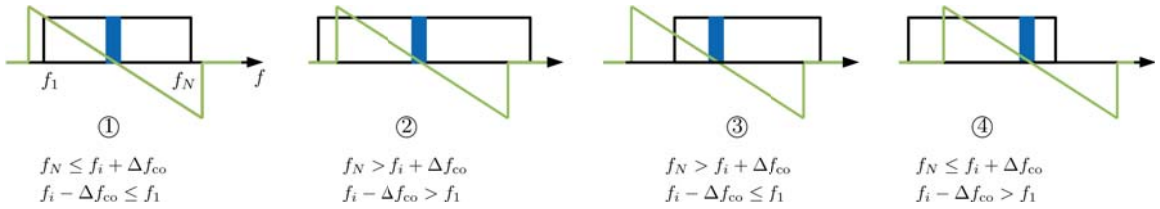

Fig. 2: Sketch of the two-sided triangular Raman window (green line) of width $2\Delta f_{\rm co}$ centered at a generic CUT frequency f_i for the scenarios in Eq. (3). The WDM central frequency is 0 by assumption.

ing. For larger bandwidths, the Raman gain is better described through the so-called *triangular* approximation[15], where the gain is treated as a linear function up to a cut-off shift $\Delta f_{\rm co}$ and forced to zero for higher frequencies, as sketched in Fig. 1. Under this approximation, the ith channel interacts with the neighboring ones only within a Raman window with two-sided bandwidth $2\Delta f_{\rm co}$, experiencing amplification/depletion from the higher/smaller frequency channels, respectively.

Unfortunately, with the triangular approximation of $\tilde{g}_r$ the total power within the Raman window does not decay anymore with the loss profile, thus breaking one of the main properties of the model in[11],[12]. Assuming that the total power in the Raman window is undepleted by SRS, we forced an exponential decay with the loss of the channel under test (CUT). We thus extended the theory in[11],[12] to a triangular $\tilde{g}_r$ profile by still exploiting the linear shape within a window. The solution maintains the formal structure of Eq. (2) while, for uniform power allocation, the Raman shaping profile $r(f_i)$ generalizes to:

$$r(f_i)=\begin{cases} P_{\rm t} f_i & \text{case } ① \\ 0 & \text{case } ② \\ \frac{P_{\rm t}}{B_{\rm t}}\left(\frac{f_i^2}{2} - f_i f_1 + \frac{f_N^2-\Delta f_{\rm co}^2}{2}\right) & \text{case } ③ \\ \frac{P_{\rm t}}{B_{\rm t}}\left(f_N f_i - \frac{f_i^2}{2} - \frac{f_1^2-\Delta f_{\rm co}^2}{2}\right) & \text{case } ④ \end{cases} \quad (3)$$

where the cases are sketched in Fig. 2. The extended $r(f)$ takes different expressions depending on the power density in the Raman window around the CUT. In the simplest case, the Raman window of the CUT encompasses the whole WDM bandwidth $B_{\rm t}$. Therefore, for these channels, the Raman gain can be safely approximated as linear and the term $r(f_i)$ reduces to $P_{\rm t} f_i$ (case ①), as in the original theory[12]. On the other hand, if the Raman window covers only an inner portion of the WDM bandwidth, $r(f_i)$ balances out to zero (case ②). For all the other scenarios, the term $r(f_i)$ takes one of the expressions labeled with ③ or ④ in Eq. (3), depending on the position of the CUT within the WDM.

Finally, to capture the interaction between SRS and the Kerr effect, we included the generalized power evolution in the GN model theory of[10] and evaluated the variance of self-phase modulation (SPM) and cross-phase modulation (XPM). The generalized SPM and XPM variance closed-form expressions relying on the novel power evolution are formally identical to Eqs. (10)–(11) of[10] with the main difference that the term indicated by T_i in[10] must be substituted with:

$$T_i = (2\alpha - C_{\rm r} P_{\rm t} f_i)^2 \to (2\alpha_i - C_{\rm r} r(f_i))^2 \,. \quad (4)$$

It is worth noting that the generalized SPM and XPM variance expressions based on Eq. (4) coincide with[10] when the condition ① of Fig. 2 is met for all the WDM channels.

In the proposed framework, a simple (yet practically useful) pre-emphasis that equalizes a fraction $\bar{k}$ of the span SRS gain can be included in Eq. (2) by substituting[16] $L_{\rm eff}(z)$ with $L_{\rm eff}(z) - \bar{k} L_{\rm eff}(L)$, L being the span length, while maintaining the profile in Eq. (3). As a result, the NLI variance $\sigma^2_{i,\ell}$ of channel i due to channel ℓ, including $\ell = i$ as SPM, can be simply multiplied by $e^{2C_{\rm r}\bar{k}L_{\rm eff}(L)r(f_\ell)}$.

Comparison with fully-numerical GN model

We tested the generalized closed-form expressions against a fully-numerical GN model. Similarly to[17], such a benchmark model is based on a numerical solution of the ODE in Eq. (1) for each channel, exploiting the true Raman gain reported in Fig. (1) and the attenuation coefficient in Fig. 3. With such profiles, we next solved the frequency/spatial integrals underpinning the numerical GN model. They were solved by the Monte Carlo method[18] and the Filon's method[16], respectively. The validity of a fully-numerical GN

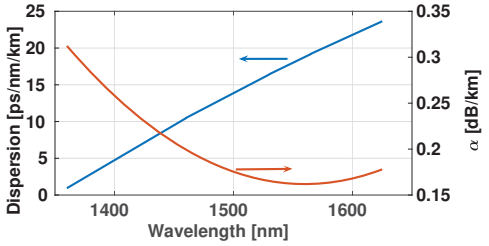

Fig. 3: Fiber dispersion coefficient (left-axis) and attenuation coefficient (right-axis) vs wavelength.

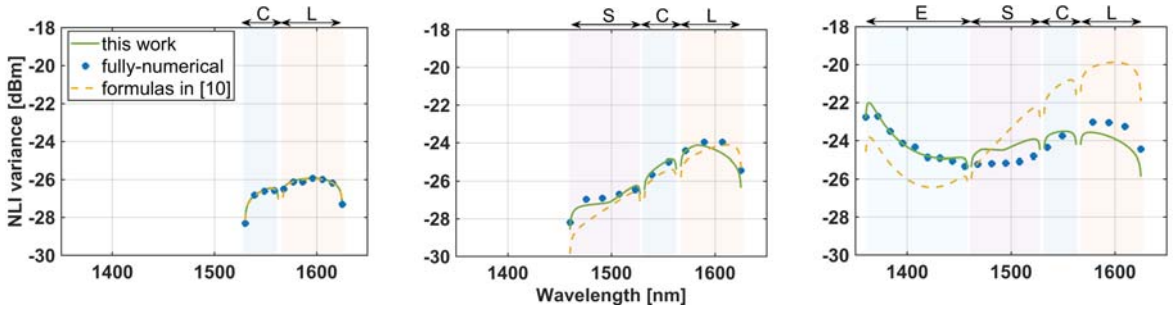

Fig. 4: NLI variance vs wavelength. From left to right: C+L, S+C+L, and E+S+C+L transmissions with channel power -1 dBm. 10 spans of SMF. Markers: fully-numerical GN model. Dashed lines: closed-form expressions in[10]. Solid lines: closed-form expressions of[10] extended through Eqs. (3)–(4).

model has been assessed in[19].

We considered a link composed of 10×100 km of single-mode fibers (SMFs) with lumped amplification and ideal power equalization at each span-end. The fiber had dispersion and attenuation coefficients reported in Fig. 3 , and nonlinear coefficient $\gamma = 1.26\ (\mathrm{W}\cdot\mathrm{km})^{-1}$. The transmitted WDM comb was a multi-band signal composed of channels modulated with Gaussian distributed symbols at symbol rate 64 Gbaud with 75 GHz spacing, and guard bands of 500 GHz.

At first, we considered the transmission of signals covering the C+L (≈11 THz), S+C+L (≈ 20 THz), and E+S+C+L bands (≈ 35 THz) at channel power -1 dBm. The results are shown in Fig. 4, where the markers indicate the fully-numerical benchmark GN model, the dashed lines indicate the GN model closed-form expressions of[10] assuming a linear Raman gain, while the solid lines are the generalized closed-form expressions of this work. In both formulas, we adopted the same channel-dependent attenuation coefficient α_i. Figure 4 (left) shows that in the C+L band the novel variance expressions coincide with those in[10], and accurately describe the SRS-induced tilt on the NLI variance. In fact, the C+L transmission is a special case of Eq. (3) where each f_i meets the condition of case ①. On the other hand, when the WDM signal covers the S+C+L bands as in Fig. 4 (center), the generalized formulas of this work are in better agreement with the fully-numerical estimation, with a root-mean-squared error (RMSE) of 0.4 dB against the 0.7 dB of the dashed line. In particular, treating the Raman gain as linear beyond its cut-off frequency results in an overestimation of the SRS for channels in the WDM edges. In fact, these edge channels are those for which case ③ or ④ in Fig. 2 applies, and hence are undergoing SRS only from a portion of the overall channels. The linear approximation of the Raman gain becomes highly detrimental for even wider bandwidths. In particular, for the E+S+C+L transmission in Fig. 4 (right), the proposed formulas allowed us to reduce the RMSE from 2 dB to 0.6 dB.

Focusing on an S+C+L transmission, we next considered different power allocations with fixed total power 24 dBm: uniform power allocation and signal-power pre-emphasis with shaping factor $\bar{k} = 0.2$. The results of the fully-numerical GN model are reported in Fig. 5 in blue circles for the uniform allocation and red triangles for the pre-emphasis. The power allocations are reported in the inset, with the same color code. The figure shows that the accuracy of the generalized model for the two cases is comparable, with RMSE of 0.4 dB and maximum gap within 1 dB.

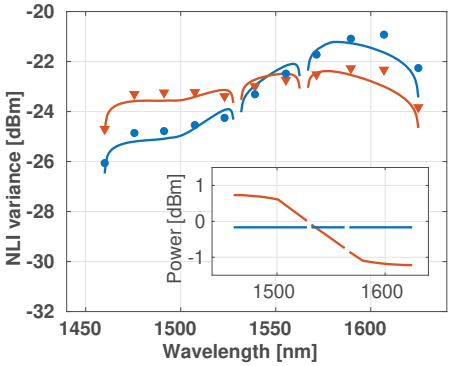

Fig. 5: NLI variance vs wavelength for an S+C+L transmission at total power 24 dBm with uniform power allocation (blue) and signal power pre-emphasis (red) with factor $\bar{k} = 0.2$. Markers: fully-numerical GN model. Solid line: extended closed-form expressions.

Conclusions

We generalized the analytical expression of the power evolution in[11],[12] to transmissions beyond the C+L band by exploiting a Raman triangular profile. We showed that, by leveraging such analytical expression, the GN model closed-form expressions of[10] can be extended to multi-band transmissions. The extended formulas can be computed in real-time and do not need extra fitting parameters to capture SRS. They can be used to analyze multi-band transmissions.

Acknowledgments

This work was supported by the Italian government through the project PRIN 2017 (FIRST).

References

[1] A. Ferrari, A. Napoli, J. K. Fischer, N. Costa, A. D' Amico, J. Pedro, W. Forysiak, E. Pincemin, A. Lord, A. Stavdas, J. P. F.-P. Gimenez, G. Roelkens, N. Calabretta, S. Abrate, B. Sommerkorn-Krombholz, and V. Curri, "Assessment on the Achievable Throughput of Multi-Band ITU-T G.652.D Fiber Transmission Systems", *J. Lightw. Technol.*, vol. 38, no. 16, pp. 4279–4291, 2020. DOI: 10.1109/JLT.2020.2989620.

[2] G. Agrawal, *Nonlinear Fiber Optics*, 3rd. San Diego, CA: Academic Press, 2001, ISBN: 0120451433.

[3] P. Serena, C. Lasagni, S. Musetti, and A. Bononi, "On Numerical Simulations of Ultra-Wideband Long-Haul Optical Communication Systems", *J. Lightw. Technol.*, vol. 38, no. 5, pp. 1019–1031, Mar. 2020. DOI: 10.1109/JLT.2019.2938580.

[4] B. Correia, R. Sadeghi, E. Virgillito, A. Napoli, N. Costa, J. Pedro, and V. Curri, "Power control strategies and network performance assessment for C+L+S multiband optical transport", *J. Opt. Commun. Netw.*, vol. 13, no. 7, pp. 147–157, 2021. DOI: 10.1364/JOCN.419293.

[5] N. Sambo, A. Ferrari, A. Napoli, N. Costa, J. Pedro, B. Sommerkorn-Krombholz, P. Castoldi, and V. Curri, "Provisioning in Multi-Band Optical Networks", *J. Lightw. Technol.*, vol. 38, no. 9, pp. 2598–2605, 2020. DOI: 10.1109/JLT.2020.2983227.

[6] P. Poggiolini, "The GN Model of Non-Linear Propagation in Uncompensated Coherent Optical Systems", *J. Lightw. Technol.*, vol. 30, no. 24, pp. 3857–3879, 2012. DOI: 10.1109/JLT.2012.2217729.

[7] M. Ranjbar Zefreh, F. Forghieri, S. Piciaccia, and P. Poggiolini, "Accurate Closed-Form Real-Time EGN Model Formula Leveraging Machine-Learning Over 8500 Thoroughly Randomized Full C-Band Systems", *J. Lightw. Technol.*, vol. 38, no. 18, pp. 4987–4999, 2020. DOI: 10.1109/JLT.2020.2997395.

[8] D. Semrau, R. I. Killey, and P. Bayvel, "The Gaussian Noise Model in the Presence of Inter-Channel Stimulated Raman Scattering", *J. Lightw. Technol.*, vol. 36, no. 14, pp. 3046–3055, 2018. DOI: 10.1109/JLT.2018.2830973.

[9] M. Cantono, D. Pilori, A. Ferrari, C. Catanese, J. Thouras, J. Augé, and V. Curri, "On the Interplay of Nonlinear Interference Generation With Stimulated Raman Scattering for QoT Estimation", *J. Lightw. Technol.*, vol. 36, no. 15, pp. 3131–3141, Aug. 2018. DOI: 10.1109/JLT.2018.2814840.

[10] D. Semrau, R. I. Killey, and P. Bayvel, "A Closed-Form Approximation of the Gaussian Noise Model in the Presence of Inter-Channel Stimulated Raman Scattering", *J. Lightw. Technol.*, vol. 37, no. 9, pp. 1924–1936, 2019. DOI: 10.1109/JLT.2019.2895237.

[11] D. N. Christodoulides and R. B. Jander, "Evolution of stimulated raman crosstalk in wavelength division multiplexed systems", *IEEE Photon. Technol. Lett.*, vol. 8, no. 12, pp. 1722–1724, Dec. 1996. DOI: 10.1109/68.544731.

[12] M. Zirngibl, "Analytical model of Raman gain effects in massive wavelength division multiplexed transmission systems", *Electron. Lett.*, vol. 34, no. 8, pp. 789–790, 1998. DOI: 10.1049/el:19980555.

[13] D. Semrau, L. Galdino, E. Sillekens, D. Lavery, R. I. Killey, and P. Bayvel, "Modulation format dependent, closed-form formula for estimating nonlinear interference in S+C+L band systems", in *45th European Conference on Optical Communication (ECOC 2019)*, 2019, paper W.1.D.1. DOI: 10.1049/cp.2019.0892.

[14] M. R. Zefreh and P. Poggiolini, "A Real-Time Closed-Form Model for Nonlinearity Modeling in Ultra-Wide-Band Optical Fiber Links Accounting for Inter-channel Stimulated Raman Scattering and Co-Propagating Raman Amplification", *arXiv*, 2020. DOI: 10.48550/ARXIV.2006.03088.

[15] A. Chraplyvy, "Optical power limits in multi-channel wavelength-division-multiplexed systems due to stimulated Raman scattering", *Electron. Lett.*, vol. 20, no. 2, pp. 58–59, 1984. DOI: 10.1049/el:19840040.

[16] C. Lasagni, P. Serena, and A. Bononi, "Modeling Nonlinear Interference With Sparse Raman-Tilt Equalization", *J. Lightw. Technol.*, vol. 39, no. 15, pp. 4980–4989, 2021. DOI: 10.1109/JLT.2021.3082287.

[17] A. Ferrari, M. Filer, K. Balasubramanian, Y. Yin, E. Le Rouzic, J. Kundrat, G. Grammel, G. Galimberti, and V. Curri, "GNPy: an open source application for physical layer aware open optical networks", *J. Opt. Commun. Netw.*, vol. 12, no. 6, pp. C31–C40, 2020. DOI: 10.1364/JOCN.382906.

[18] R. Dar, M. Feder, A. Mecozzi, and M. Shtaif, "Accumulation of nonlinear interference noise in multi-span fiber-optic systems", *Opt. Express*, vol. 22, no. 12, pp. 14 199–14 211, Jun. 2014. DOI: 10.1364/OE.22.014199.

[19] A. D'Amico, L. Guyader, F. Frank, E. Le Rouzic, E. Pincemin, A. Napoli, H. Sun, B. Spinnler, N. Brochier, and V. Curri, "GNPy Experimental Validation for Nyquist Subcarriers Flexible Transmission up to 800 G", in *2022 Optical Fiber Communications Conference and Exhibition (OFC)*, 2022, paper M4F.6. DOI: 10.1364/OFC.2022.M4F.6.